Pressure-induced structural phase transition in the Bechgaard-Fabre salts

A. Pashkin[a], M. Dressel[b], S.G. Ebbinghaus[c], M. Hanfland[d], C.A. Kuntscher[a,*]

[a] *Experimentalphysik II, Universität Augsburg, Universitätsstr. 1, 86159 Augsburg, Germany*
[b] *1. Physikalisches Institut, Universität Stuttgart, Pfaffenwaldring 57, 70550 Stuttgart, Germany*
[c] *Martin-Luther-Universität Halle-Wittenberg, Institut für Chemie, Kurt-Mothes-Straße 2, 06120 Halle, Germany*
[d] *European Synchrotron Radiation Facility, BP 220, 38043 Grenoble, France*

1. Introduction

The Fabre salts $(TMTTF)_2X$ and the Bechgaard salts $(TMTSF)_2X$ represent prime examples of quasi-one-dimensional electronic systems demonstrating a large variety of phenomena such as superconductivity, charge order, Mott–Hubbard insulating state, spin-density-waves etc. which have been extensively studied over the last three decades [1–4]. The structure of these salts consist of molecular stacks formed by tetramethyltetrathiafulvalene (TMTTF) or tetramethyltetraselenafulvalene (TMTSF) cations separated by the monovalent X^- anions. At room temperature, the $(TMTTF)_2X$ salts are typically Mott–Hubbard insulators due to the strong correlation of electrons and a weak interchain coupling [5]. On the other hand, the $(TMTSF)_2X$ salts are good quasi-one-dimensional metals although their properties are still strongly affected by correlation effects [4,6].

In the Bechgaard-Fabre salts the interstack separation and therefore the interchain hopping integral can be nicely tuned either by changing the size of the X^- anions or the type of the cation (chemical pressure effect), or by applying external pressure. It has been demonstrated that the effect of chemical and external hydrostatic pressure are virtually equivalent; i.e. numerous physical quantities of $(TMTSF)_2X$ resemble those of $(TMTTF)_2X$ under pressure. This provides the possibility to construct a generic temperature–pressure phase diagram [7,8] of the Bechgaard-Fabre salts. Continuous tuning of external pressure and temperature is the best way to explore the phase boundaries in this diagram. Employing a diamond anvil cell (DAC) to generate extreme pressures made it possible, for instance, to tune $(TMTTF)_2PF_6$ throughout the phase diagram starting from the insulating spin-Peierls up to the superconducting state [9–11]. A DAC has also been used in infrared spectroscopy experiments that demonstrated pressure-induced insulator-to-metal transition in the TMTTF family [12,13]. For a correct quantitative analysis of data obtained in the above mentioned experiments, knowledge of the crystal structure is crucial. However, the compressibility and structure at high pressures of the Bechgaard-Fabre salts has not been measured up to the present day. To the best of our knowledge, the highest pressure at which the structure has been determined is 1.6 GPa for the example of $(TMTSF)_2PF_6$—the first organic superconductor [14,15]. On the other hand, high-pressure dc transport of $(TMTTF)_2PF_6$ has been investigated at pressures up to 8 GPa [10], much higher than any structural study of the Bechgaard-Fabre salts reported up to now.

In this paper, we present results of single-crystal X-ray diffraction performed on two typical salts $(TMTTF)_2PF_6$ and $(TMTSF)_2PF_6$ for pressures up to 10 GPa. We determine the pressure dependence of the unit-cell constants and volume compressibility of the crystals. Moreover, we found pressure-induced structural phase transitions which take place at high pressures in both studied salts.

2. Experiment

Single crystals of $(TMTTF)_2PF_6$ and $(TMTSF)_2PF_6$ were grown by a standard electrochemical procedure [16]. The room-temperature

* Corresponding author. Tel.: +49 (0)821 598 3315; fax: +49 (0)821 598 3411.
E-mail address: christine.kuntscher@physik.uni-augsburg.de (C.A. Kuntscher).

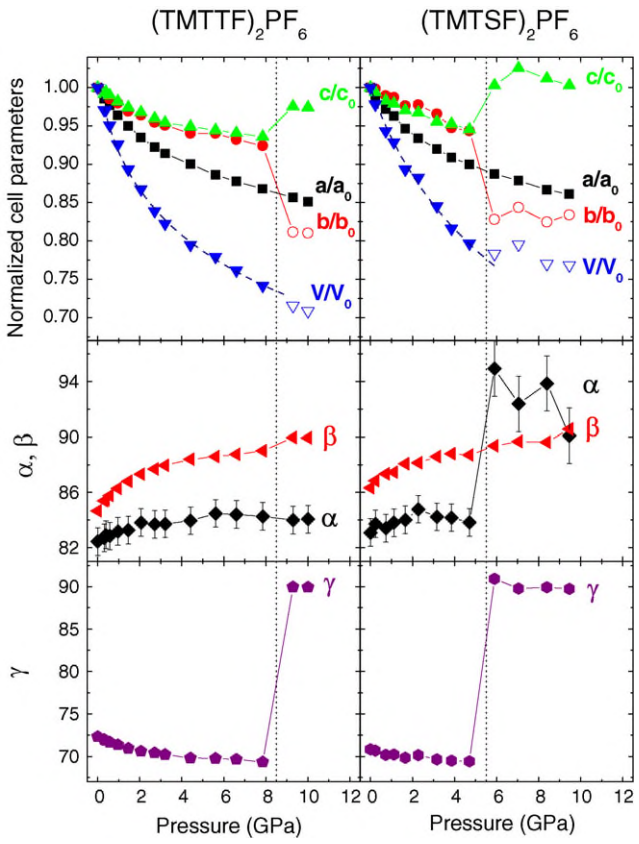

Fig. 1. (Color online) Unit-cell parameters of $(TMTTF)_2PF_6$ and $(TMTSF)_2PF_6$ as a function of pressure obtained at room temperature. Vertical dotted lines mark the transition pressure P_c. Open symbols correspond to the values of the parameter b and the unit-cell volume V multiplied by the factor 1/2 in the high-pressure phase. The dashed blue lines correspond to the fit of the pressure-dependent unit-cell volume below P_c using the Birch Eq. (1).

X-ray diffraction experiments were carried out at beamline ID09A of the European Synchrotron Radiation Facility in Grenoble. The wavelength used for the experiments was 0.413 Å. X-ray diffraction patterns were collected on an image plate MAR345 detector. The DAC rotation angle varied from -30° to $+30^\circ$ for $(TMTTF)_2PF_6$ and from -20° to $+20^\circ$ for $(TMTSF)_2PF_6$ with 2° step. Liquid helium served as pressure transmitting medium in the DAC. The diffraction patterns have been analyzed using the XDS package [17]. The pressure in the DAC was determined *in situ* by the ruby luminescence method [18].

3. Results and discussion

The single-crystal X-ray diffraction analysis confirms the space-group symmetry $P\bar{1}$ of both studied compounds in the low-pressure phase reported previously [19,14]. The pressure dependence of the normalized cell parameters of $(TMTTF)_2PF_6$ and $(TMTSF)_2PF_6$ compounds is shown in Fig. 1. The compression of both compounds is anisotropic: The *intrastack* molecular separation defined by the unit-cell parameter a suffers an approximately two times larger variation under pressure compared to the b and c-axes lattice parameters, which are related to the *i*nterstack separation. This is in qualitative agreement with the first high-pressure X-ray diffraction study of the $(TMTSF)_2PF_6$ salt by Morosin et al. [20] and in quantitative agreement with a later, more detailed study of Gallois et al. [14,15]. Furthermore, the maximum softness in the stacking direction is in accord with the anisotropy of the thermal expansion coefficient that is largest along the a axis [14,21].

Table 1
The unit-cell parameters of $(TMTTF)_2PF_6$ and $(TMTSF)_2PF_6$ at ambient pressure and above the transition pressure.

	$(TMTTF)_2PF_6$		$(TMTSF)_2PF_6$	
	$P = 0$ GPa	$P = 9$ GPa	$P = 0$ GPa	$P = 5.9$ GPa
a (Å)	7.16	6.13	7.28	6.46
b (Å)	7.57	12.29	7.68	12.72
c (Å)	13.21	12.89	13.49	13.53
α	82.4	84.0	83.1	95.6
β	84.7	90.0	86.3	89.5
γ	72.3	90.0	70.8	90.9
V_0 (Å^3)	675.0	965.8	706.9	1101
B_0 (GPa)	7.27 ± 0.64	–	12.71 ± 0.97	–
B_0'	9.98 ± 1.15	–	4.23 ± 0.75	–

The bulk modulus B_0 and its pressure derivative B_0' obtained from the fit according to Eq. (1) are given for the low-pressure phase.

The change of the unit-cell volume can be well fitted with the Birch equation of state [22]:

$$P(V) = \frac{3}{2}B_0(x^7 - x^5)\left[1 + \frac{3}{4}(B_0' - 4)(x^2 - 1)\right] \quad (1)$$

with $x = (V_0/V)^{1/3}$, where V_0 is the unit-cell volume at ambient pressure; B_0 denotes the bulk modulus and B_0' its pressure derivative. The parameters of the fit together with the absolute values of the unit-cell dimensions are given in Table 1. The values reported for $(TMTSF)_2PF_6$ are in reasonable agreement with previous structural studies under moderate pressure [14,15].

Upon increasing the pressure further, the unit-cell parameters experience an abrupt jump indicating a pressure-induced structural phase transition. The transition occurs at 5.5 GPa in $(TMTSF)_2PF_6$ and at 8.5 GPa in $(TMTTF)_2PF_6$. These critical pressures are marked in Fig. 1 by vertical dotted lines. The most salient changes across the transition are the doubling of the unit cell along the b axis (Like the unit cell volume, in Fig. 1 the lattice parameter b is thus scaled by a factor of 0.5 above the transition.) and the increase of the angle γ to 90°. Another noticeable anomaly of approximately 5% occurs in the lattice parameter c. Simultaneously, the parameters β and a do not reveal any discontinuity within the precision of the experimental data. In case of $(TMTTF)_2PF_6$ the angle α remains at the value of about 84° above the transition, but it abruptly increases to values above 90° in the case of $(TMTSF)_2PF_6$. At present, it is not clear, whether the anomaly in α observed for $(TMTSF)_2PF_6$ is a real effect or due to the lower quality of the diffraction pattern in the high-pressure phase. Since for both organic salts α deviates from 90° above P_c, in contrast to β and γ, the crystal symmetry of the high-pressure phase should be specified as monoclinic. This seems to be a stable configuration that does not change with pressure any more.

We suggest a tentative model illustrated in Fig. 2 to explain the pressure-induced structural distortion. By looking along the c axis, the figure basically shows the projection of the crystal structure onto the ab plane for pressures below and above the transition P_c. The fluorine and hydrogen atoms are not shown for simplicity. The initial compression of the crystal lattice pushes the molecular stacks of cations closer to each other. This effect is in particular strong along the b axis, since the interstack separation is already small at ambient pressure compared to the separation in c^* direction. Above the critical pressure P_c the interstack interaction becomes strong enough to drive the structural instability. It leads to a small tilting of the cation molecules in the stacks such that two neighboring unit cells become inequivalent. As a result the unit cell doubles and the new unit cell translational vector b is defined as shown in Fig. 2(c). However, we have to stress that although the unit-cell parameters depicted in Fig. 2 corresponds to our experimental data taken for the $(TMTSF)_2PF_6$ sample, the

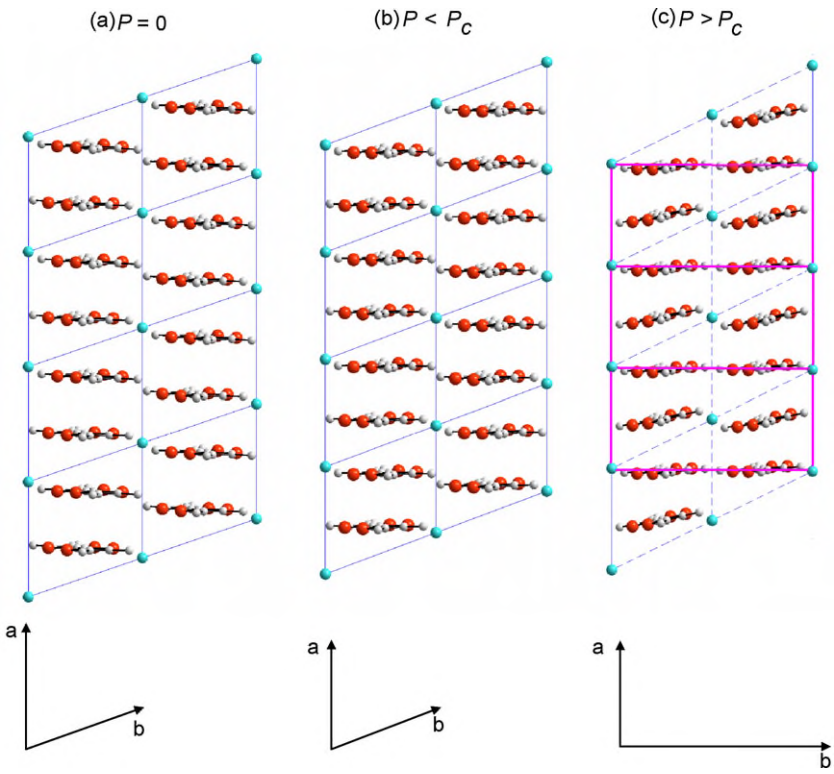

Fig. 2. (Color online) Illustration of the changes in the crystal structure of the Bechgaard-Fabre salts across the structural phase transition. (a) Crystal structure at ambient pressure; (b) compressed structure just below the transition pressure P_c; (c) new structural phase stabilized above the transition pressure P_c. Arrows depict translation vectors.

atomic positions could not be unambiguously extracted from the X-ray diffraction data and, therefore, the depicted structural distortion is only schematic.

The unit-cell parameters of the high-pressure phase are directly related to the unit-cell parameters in the low-pressure phase according to:

$$b^* = \sqrt{a^2 + 4b^2 - 4ab\cos\gamma},$$
$$\gamma^* = 180 - \arcsin\left(\frac{2b\sin\gamma}{b^*}\right). \quad (2)$$

Thus, in order to verify the occurrence of a structural phase transition and to rule out that the observed anomalies are only due to a redefinition of the unit cell, we convert the unit-cell parameters in the low-pressure phase according to Eq. (2) and compare them with the corresponding values above P_c. Fig. 3 shows such a comparison of b^* and γ^* for both studied salts. One clearly observes discontinuities in b^* and γ^* which characterizes the type of the structural phase transition as first order.

The reason for the unit cell doubling and formation of the quasi-orthorhombic structure could be the enhancement of the interaction between the cation molecules in the stacks and the anions, which becomes particularly strong for $\gamma^* = 90^\circ$, i.e., when the planar cation molecules and the anions are arranged within the same crystallographic plane.

Remarkably, the pressure offset between the structural transitions in $(TMTTF)_2PF_6$ compared to $(TMTSF)_2PF_6$ is about 3 GPa, i.e., almost exactly the same as the offset between electronic phases of both compounds in the generic phase diagram of the Bechgaard-Fabre salts. [7] However, it seems unlikely that the structural distortion is related to some kind of electronic instability, since in this case the spectrum of electronic excitations would change. This is, however, not observed in infrared spectra of $(TMTSF)_2PF_6$ above the structural transition, i.e., for $P > 5.5$ GPa. The reflectivity along the a and b' direction shows a metallic character with a rather small anisotropy. No indication of an energy gap and other sudden changes was observed [13].

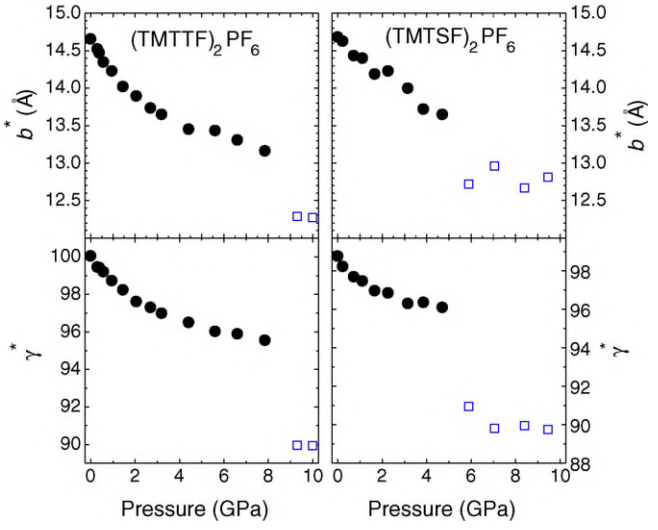

Fig. 3. (Color online) The parameters b^* and γ^* for the monoclinic unit cell of $(TMTTF)_2PF_6$ and $(TMTSF)_2PF_6$ as a function of pressure up to 10 GPa. Open symbols: Values of the parameters in the high-pressure phase directly obtained from the X-ray diffraction analysis. Full symbols: Values of the cell parameters in the low-pressure phase, calculated according to Eq. (2) for the redefined unit cell.

4. Summary

We performed room temperature X-ray diffraction study under pressure of the quasi-one-dimensional salts $(TMTTF)_2PF_6$ and $(TMTSF)_2PF_6$. The pressure dependence of the unit-cell constants has been obtained for pressures up to 10 GPa. A structural phase

transition from a triclinic to a *monoclinic* phase is observed at 5.5 and 8.5 GPa in $(TMTSF)_2PF_6$ and $(TMTTF)_2PF_6$, respectively. The transition is accompanied by a doubling of the unit cell along the b axis. Several unit-cell parameters (b^*, γ^* and c) show a considerable discontinuity across the transition pressure indicating a first-order phase transition. A tentative model of the structural distortion related to the modulation of the cation tilting in the stacks is proposed.

Acknowledgements

We would like to thank G. Untereiner for crystal growth and N. Drichko, M. Dumm and E. Rose for fruitful discussions and comments. We acknowledge the ESRF facility for the provision of beamtime. Financial support is provided by the DFG (Emmy-Noether program, SFB 484, DR228/27).

References

[1] D. Jérome, H.J. Schulz, Adv. Phys. 31 (1982) 299.
[2] T. Ishiguro, K. Yamaji, G. Saito, Organic Superconductors, Springer, Berlin, 1998.
[3] D. Jerome, Chem. Rev. 104 (2004) 5565.
[4] M. Dressel, Naturwissenschaften 90 (2003) 337.
[5] T. Giamarchi, Chapter from Luttinger to fermi liquids in organic conductors, in: The Physics of Organic Superconductors and Conductors, vol. 110, Springer, Berlin Heidelberg, 2008, pp. 719–743.
[6] M. Dressel, A. Schwartz, G. Grüner, L. Degiorgi, Phys. Rev. Lett. 77 (1996) 398.
[7] C. Bourbonnais, D. Jérome, Science 281 (1998) 1155.
[8] H. Wilhelm, D. Jaccard, R. Duprat, C. Bourbonnais, D. Jérome, J. Moser, C. Carcel, J.M. Fabre, Eur. Phys. J. B 21 (2001) 175.
[9] T. Adachi, E. Ojima, K. Kato, H. Kobayashi, T. Miyazaki, M. Tokumoto, A. Kobayashi, J. Am. Chem. Soc. 122 (2000) 3238.
[10] D. Jaccard, H. Wilhelm, D. Jérome, J. Moser, C. Carcel, J.M. Fabre, J. Phys.: Condens. Matter 13 (2001) L89.
[11] C. Araki, M. Itoi, M. Hedo, Y. Uwatoko, H. Mori, J. Phys. Soc. Jpn. 76SA (2007) 198.
[12] A. Pashkin, M. Dressel, C.A. Kuntscher, Phys. Rev. B 74 (2006) 165118.
[13] A. Pashkin, M. Dressel, M. Hanfland, C.A. Kuntscher, to be published.
[14] B. Gallois, J. Gaultier, C. Hauw, T.-D. Lamcharfi, Acta Cryst. B 42 (1986) 564.
[15] B. Gallois, J. Gaultier, T. Lamcharfi, F. Bechtel, A. Filhol, L. Ducasse, M. Abderrabba, Synth. Met. 19 (1987) 321.
[16] L.K. Montgomery, Organic Conductors, Marcel Dekker, New York, 1994.
[17] W. Kabsch, J. Appl. Cryst. 26 (1993) 795.
[18] H.K. Mao, J. Xu, P.M. Bell, J. Geophys. Res. 91 (1986) 4673.
[19] P. Delhaes, C. Coulon, J. Amiell, S. Flandrois, E. Torreilles, J.M. Fabre, L. Giral, Mol. Cryst. Liq. Cryst. 50 (1979) 43.
[20] B. Morosin, J.E. Schirber, R.L. Greene, E.M. Engler, Phys. Rev. B 26 (1982) 2660.
[21] M. de Souza, P. Foury-Leylekian, A. Moradpour, J.-P. Pouget, M. Lang, Phys. Rev. Lett. 101 (2008) 216403.
[22] F. Birch, J. Geophys. Res. 83 (1978) 1257.